DEFORMATION MONITORING OF TURTLE MOUNTAIN BY HIGH-PRECISION PHOTOGRAMMETRY

Report 1-83

Alberta

85-1511/

RESEARCH MANAGEMENT DIVISION LOGO

The logo represents the interdisciplinary and holistic nature of the Division's environmental research programs. Each of the five sections of the symbol represent comprehensive programs on air, water, land, humans and their constant interaction. The sections converge to form a cohesive chain, characteristic of an effective research organization. This cohesive bonding makes the sections blossom into the environment in the form of a flower — an Albertan wild rose.

DEFORMATION MONITORING OF TURTLE MOUNTAIN BY HIGH-PRECISION PHOTOGRAMMETRY

Final Report

RESEARCH MANAGEMENT DIVISION
Alberta Environment

For further information on reports published by the Research Management Division, contact:

Research Management Division
Publications Office
14th Floor, Standard Life Centre
10405 Jasper Avenue
Edmonton, Alberta
T5J 3N4

(403) 427-3946

This report has received external peer review.

This report may be cited as:

Fraser, C.S. 1983. Deformation monitoring of Turtle Mountain by high-precision photogrammetry. Prep. for Alberta Environment, Research Management Division by University of Calgary, Division of Surveying Engineering. Edmonton, Alberta: Research Management Division. Report L-83. 42 pp.

DEFORMATION MONITORING OF TURTLE MOUNTAIN BY HIGH-PRECISION PHOTOGRAMMETRY

by

C.S. FRASER, P.Eng.

Division of Surveying Engineering
The University of Calgary

for

RESEARCH MANAGEMENT DIVISION

Alberta Environment

Report L-83

November 1983

This report is made available as a public service. The Department of Environment neither approves nor disagrees with the conclusions expressed herein, which are the responsibility of the author.

TABLE OF CONTENTS

		Page
LIST OF TABLES		vi
LIST OF FIGURES		vii
ABSTRACT		ix
ACKNOWLEDGEMENTS		x
1.	INTRODUCTION	1
2.	PROJECT ACTIVITIES	5
2.1	What Is Analytical Photogrammetry?	5
2.2	Photogrammetric Network Design and Sensitivity Analysis	9
2.2.1	Network Design	10
2.2.2	Sensitivity Analysis	13
2.3	Object Point Targetting and Control Survey	16
2.4	Photography	18
2.4.1	Epoch 1 (1982)	18
2.4.2	Epoch 2 (1983)	21
2.5	Photogrammetric Point Mensuration	21
2.6	Adjustment of Photogrammetric Networks	22
2.7	Deformation Analysis	26
2.7.1	The Global Congruency Test	28
2.7.2	Localization of Deformations in Space and Time	31
2.7.3	Combined Adjustment of Both Photogrammetric Networks	34
2.7.4	Strain Analysis	35
2.8	Interpretation of Results	38
3.	CONCLUSIONS	40
4.	RECOMMENDATIONS	41
5.	REFERENCES CITED	42

LIST OF TABLES

		Page
1.	Bundle Adjustment Results for the Simulated Turtle Moutain Photogrammetric Monitoring Network	14
2.	Magnitudes of Critical Point Movements Corresponding to the Five Deformation Models	15
3.	Summary of Photogrammetric Free-network Adjustment Results of Epochs 1 and 2	25
4.	Adjusted X, Y, and Z co-ordinates of the 20 Photogrammetric Target Points at Epoch 1, with Their Standard Errors	27
5.	Summary of Deformation Analysis Results for Epoch 2 Versus Epoch 1	33

LIST OF FIGURES

		Page
1.	Location Map of Frank Slide	2
2.	Photogrammetric Imaging Geometry	6
3.	Simulated Photogrammetric Network for the Monitoring of Turtle Mountain	12
4.	Photogrammetric Target Array and Camera Station Locations at Epoch 1	19
5.	Photogrammetric Imaging Geometry for Epoch 2	23
6.	"Deformations" in the Horizontal Plane, as Determined by the Localization Procedure	29
7.	"Deformations" in the Vertical Direction, as Determined by the Localization Procedure	30
8.	Point Movements in the Horizontal Plane, as Determined in the Combined Network Adjustment	36
9.	Point Movements in the Vertical Direction, as Determined in the Combined Network Adjustment	37

ABSTRACT

The development and implementation of a high-precision photogrammetric deformation monitoring system for the South Peak of Turtle Mountain, Alberta, is reported. Developmental aspects including network design, adjustment, and sensitivity analysis, as well as the analysis procedures for the detection and localization of deformations are detailed. The practical implementation of the system is outlined. This involved photogrammetric measurements at two epochs, one year apart. Results of the analysis of the photogrammetric data, which indicate that point movements on Turtle Mountain can be measured to centimetre accuracy from conventional low-level aerial photography, are discussed.

ACKNOWLEDGEMENTS

The success of this research endeavour is due in no small measure to a number of people who contributed both directly and indirectly to it. At the feasibility study level, useful discussions were held with Drs. D.M. Cruden and W. Niemeier, and Messrs. D.T. Sneddon and W. Teskey. For their assistance at the fieldwork stage, and for their continued interest in the project, the author wishes to thank Dr. E.G. Anderson and Mr. D.W. Prosser. Messrs. PC. Stoliker, J. English, and D. Skea contributed to the data acquisition and processing phases, while the deformation localization procedure was implemented by Dr. L. Gruendig. The Scientific Authority, initially Mr. D.T. Sneddon, followed by Ms. C. Jardine, was always available for encouragement and assistance.

This work was supported through a research contract with the Research Management Division of Alberta Environment. Preliminary work on the Turtle Mountain photogrammetric monitoring study was also supported by the Natural Sciences and Engineering Research Council of Canada.

1. INTRODUCTION

Just over 80 years ago, the famous Frank Slide occurred in the Crowsnest Pass in southern Alberta. This major landslide comprised some 30 million cubic metres of rock which moved down the east face of Turtle Mountain and buried a town and approximately three square kilometres of the surrounding Crowsnest Valley to an average depth of about 14 m (see location map, Figure 1). For geological and geotechnical details of the Frank Slide, the reader is referred to Cruden and Krahn (1978).

Since 1933, a number of deformation monitoring surveys have been carried out at the crown of the Frank Slide. In recent years these in situ displacement measurements have been directed at ascertaining the stability of a five million cubic metre rock wedge which comprises the South Peak area of Turtle Mountain. The principal geotechnical hypothesis regarding the potentially hazardous movement of this pyramid block is that it will move eastward, thus causing a dilation at the gaping fissure which defines the western edge of the wedge. This fissure, called Crack 1, is capable of detecting movements to a high accuracy, it does display a few drawbacks. First, only movement across or along Crack 1 can be monitored and, second, if hazardous movements occur and these indicate potential structural failure, it will no longer be possible to safely carry out in situ measurements.

High-precision photogrammetry is a measuring tool which is well suited to a deformation monitoring task such as Turtle Mountain, since it is both non-contact in nature and also capable of yielding a comprehensive picture of the rock displacement pattern over the entire summit ridge area. At the invitation of the Alberta Department of Environment, the author conducted a comprehensive study to ascertain whether analytically restituted low-level aerial photography could be used to measure sub-centimetre rock movements on the South Peak. From the results of the study it was concluded that a photogrammetric measuring system was a feasible option for monitoring deformations on Turtle Mountain. Consequently the decision was made to develop and implement such a system.

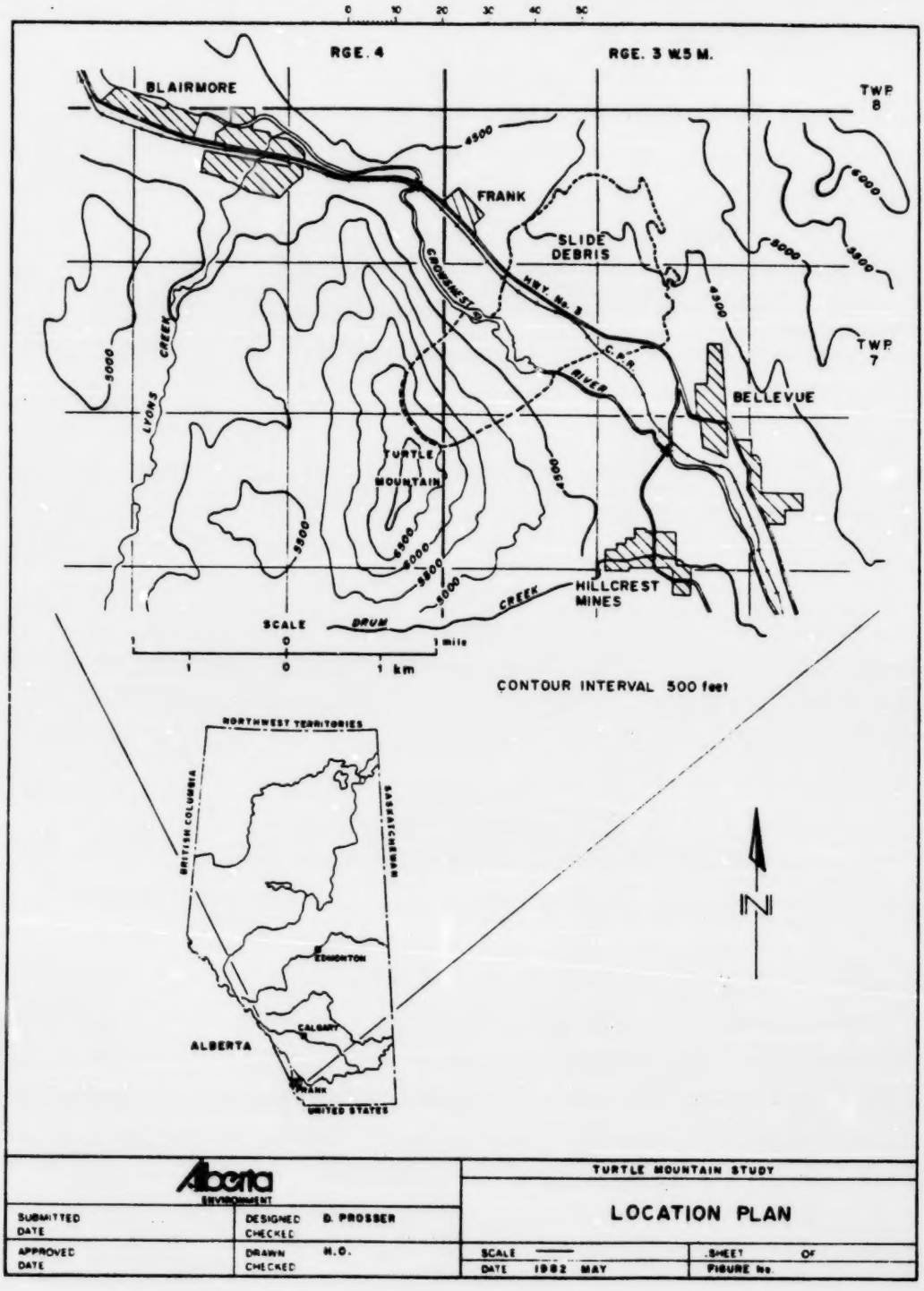

Figure 1. Location map of Frank Slide.

This report details the research work carried out for Alberta Environment, Research Management Division. The overall purpose of the research was to develop, test, and implement a photogrammetric monitoring system for the South Peak of Turtle Mountain that would be capable of detecting multi-point movements to an accuracy level of one centimetre.

The research work basically covered a period of design and development of the proposed photogrammetric system, coupled with simulation studies. This initial phase was then followed by two epochs of photogrammetric measurements of the South Peak of Turtle Mountain. The first epoch of photography occurred in late summer of 1982, followed by a further aerial photographic mission in August 1983. From the changes in position of object space target points between epochs 1 and 2, the pattern of deformation of the summit ridge area was determined.

In the individual research phases, the following seven principal activities were involved in the project:

1. photogrammetric network design and sensitivity analysis;
2. object point targetting and control survey;
3. photography;
4. photogrammetric point mensuration;
5. network adjustment;
6. deformation analysis; and
7. interpretation of results.

In Section 2, these seven work phases are discussed under separate headings. In each subsection, a general overview of salient aspects is first given, followed by a specific account of the procedures adopted for the photogrammetric monitoring of Turtle Mountain. Also, where applicable, the results obtained in each work activity are presented and discussed. Conclusions drawn from the research carried out thus far are summarized in Section 3, and general recommendations pertaining to a possible continuation of the photogrammetric monitoring program are presented in Section 4.

In many respects the photogrammetric system developed and implemented for the monitoring of Turtle Mountain is unique. To the

author's knowledge, this high-precision measuring and deformation analysis project is the first of its kind to be conducted in Canada. Furthermore, certain aspects of the data analysis, notably the rigorous sensitivity and deformation analyses, have not been applied previously in analytical photogrammetric monitoring schemes.

In the main body of this report an attempt is made to present the theoretical concepts involved in the research in a non-mathematical manner in order to enhance general readability. For the reader seeking a more detailed account of the mathematical background, an external appendix has been provided (published separately as RMD Report OF-62). This appendix includes seven photocopies of relevant publications (two deal specifically with the Turtle Mountain investigation) as well as a writeup on one of the software packages developed.

2. PROJECT ACTIVITIES

2.1 WHAT IS ANALYTICAL PHOTOGRAMMETRY?

Prior to discussing each of the project activities, a brief answer to the question of what analytical photogrammetry is will be offered.

Photogrammetry is defined as the art, science, and technology of obtaining reliable information about physical objects and the environment through processes of recording, measuring, and interpreting images and patterns of electromagnetic radiant energy and other phenomena. One of the many diverse fields of photogrammetry, in which advances in both theory and digital techniques have had a profound influence over the last decade, is non-topographic photogrammetry. Principally as a result of the increased flexibility and accuracy afforded by analytical methods, photogrammetry has evolved from a topographic mapping tool into a precise measurement technique which nowadays finds application in areas such as engineering, industry, and medicine. The term non-topographic photogrammetry covers conventional and non-conventional imaging techniques such as close-range, underwater, and terrestrial photogrammetry.

The photographic image of an object target array represents a perspective projection of the three-dimensional scene being imaged onto a two-dimensional plane, the focal plane of the camera. The analytical restitution process is then the mathematical reconstruction of the three-dimensional object space from two-dimensional measurements on two or more overlapping photographs. Referring to Figure 2, this process entails the determination of the object space (X,Y,Z) co-ordinates of the target point J through the spatial intersection of the three imaging rays shown in the figure. That is, using the image space (x,y) co-ordinates of point j on each of the photographs, an image-to-object space transformation is carried out according to the relationships of projective geometry. The inverse transformation (i.e., from object to image space) also plays a significant role in analytical restitution.

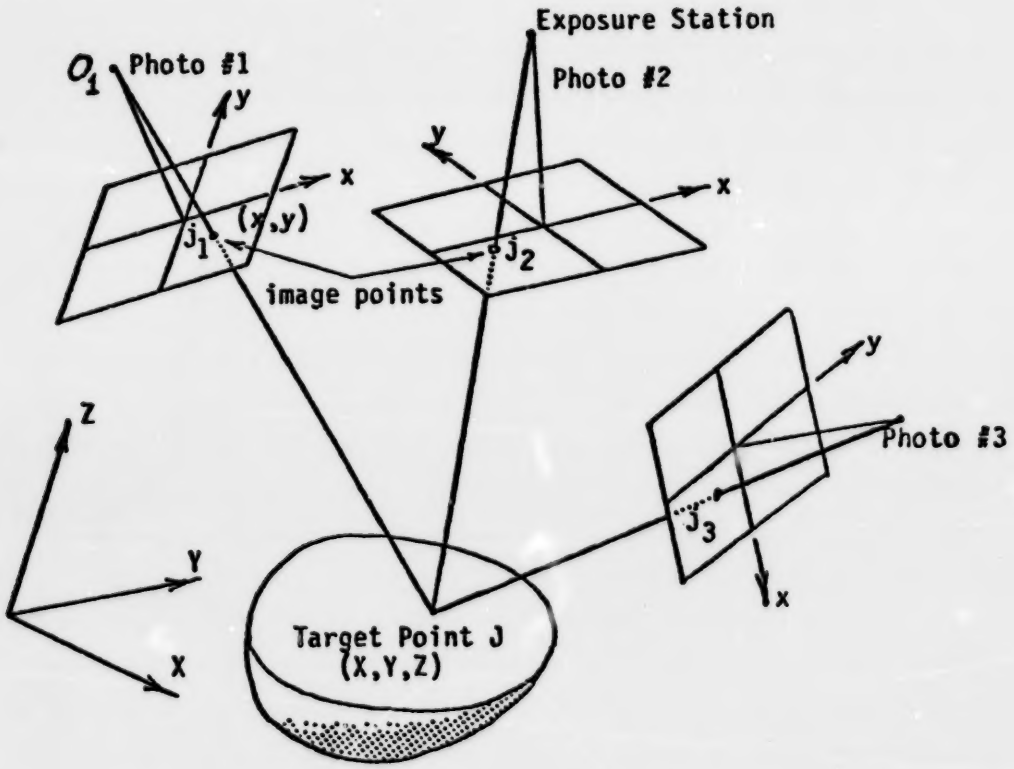

Figure 2. Photogrammetric imaging geometry.

The analytical restitution process can be carried out in either a sequential or "simultaneous" manner. With the sequential approach, a control field of points with known (X,Y,Z) co-ordinates is established and space resections are carried out, based on this fixed control, to determine the spatial position O_i and attitude (orientation) of each photograph. Having established the exterior orientation parameters for each image, all rays O_iJ_i (see Figure 2) are defined and thus the target point J can be obtained by space intersection. Although the sequential method yields some insight into the restitution process, it is inappropriate for high-precision measuring, especially in cases where an object space array of surveyed control points is not established.

The most appropriate "simultaneous" restitution method for high-precision deformation surveys is the bundle adjustment. With this approach, all photogrammetric system unknowns (i.e., object space [X,Y,Z] co-ordinates, exterior and interior orientation elements, and self-calibration parameters) are recovered simultaneously. Without going into detail, the linear functional model fo the bundle adjustment is given by the observation equation

$$\underline{v} = \underline{A}_1 x_1 + \underline{A}_2 \underline{x}_2 + \underline{A}_3 \underline{x}_3 - (\ell - \underline{F}^\circ) \qquad (1)$$

where the parameter vectors $\underline{x}_1$ represent the following unknowns: $\underline{x}_2$ the object space (X,Y,Z) co-ordinates of target points; $\underline{x}$ the position and attitude of each photograph in the (X,Y,Z) system; and $\underline{x}_3$ the self-calibration and interior orientation parameters for the imaging camera or cameras. The vector ℓ represents the photogrammetric (x,y) data measurements, $\underline{v}$ is a vector of residuals, and $\underline{F}^\circ$ a vector of approximate values. The matrices $\underline{A}_1$, A_2, and $\underline{A}_3$ are design matrices. In addition to the linear functional model, certain stochastic properties of the observations are modelled, and the final photogrammetric adjustment that yields the parameter estimates is carried out according to the standard least-squares method.

As regards the accuracy potential of analytical photogrammetry, in aerial triangulation adjustments accuracy is most often assessed by

the comparison of photogrammetrically determined co-ordinates with "true" checkpoint co-ordinates. However, in the absence of independent object space measurements of significantly higher accuracy, one must turn to measures of statistical precision. In the case of the bundle adjustment, the covariance matrix $\underline{C}_{x_2}$ provides a measure of the overall object point accuracy. As a non-number summary, the global "mean" standard error $\bar{\sigma}_c$ of the object point (X,Y,Z) co-ordinates may be used:

$$\bar{\sigma}_c = \left(\frac{1}{3n} \text{ tr } \underline{C}_{x_2}\right)^{\frac{1}{2}} \qquad (2)$$

where n is the number of points and tr is the trace operator (i.e., the sum of the leading diagonal terms). Object space co-ordinate precision can also be expressed in terms of a fraction of the object field diameter in order to give a proportional accuracy measure, although such an indicator does have limitations in meaning. In the areas of high-precision engineering measurement, such as in the calibration of radar dishes by photogrammetry, accuracies of 1 part in 100 000 have been attained. However, the expected accuracy level is more commonly in the range of 1:40 000 to 1:60 000. For the analysis of deformations, the provision of $\underline{C}_{x_2}$ is critical, as all accuracy information concerning the co-ordinates $\underline{x}_2$ of points being monitored is contained in this matrix.

Turning now to areas of application, as a non-destructive, non-contact, three-dimensional measuring tool, analytical close-range photogrammetry is a particularly useful technique for the measurement of:

1. irregular shapes and surfaces;
2. inflated shapes;
3. moving objects; and
4. objects that are too hot or cold, too delicate, and too toxic or inaccessible.

Among the many recently reported applications of precise analytical non-topographic photogrammetry are the following:

1. the monitoring of construction and the measurement of volumes of spherical LNG tanks on gas vessels;

2. monitoring stability and determining deformations in earth walls, retaining walls, rock faces, and excavated areas in open cut mining;
3. shape determinations in construction engineering (e.g., cooling towers, shipbuilding, precast bridge segments, and offshore oil platforms);
4. deformation surveys of structures under static and dynamic loading (e.g., transmission lines and towers, bridges);
5. very high accuracy surveys for radar antennae calibration and jig deformation studies in aircraft assembly; and
6. long-term stability monitoring of dams and earthworks.

As a deformation monitoring system, analytical photogrammetry offers a few unique advantages over other direct measuring approaches. In cases where structures are loaded to failure or where hazardous movements are expected, the non-contact feature of photogrammetric measurements is particularly beneficial. Further, there are few limitations in the number of object points employed. For example, it is immaterial as far as the photogrammetric field work is concerned whether there are 10 or 100 targetted points at which movement is to be measured, as long as all points are imaged on a sufficient number of photographs. On the other hand, one extensometer reading yields a single distance (or change of distance) observation and points in a geodetic network need to be "tied in" by physically setting up an instrument or target over that point.

2.2 PHOTOGRAMMETRIC NETWORK DESIGN AND SENSITIVITY ANALYSIS

Prior to conducting a photogrammetric survey, the network design must be considered. In the case of Turtle Mountain, an analytical pre-analysis procedure was employed to verify that the levels of precision and sensitivity sought would be achieved with the proposed design of the photogrammetric network. The fundamental criterion governing the selection of such factors as the number and geometry of the camera stations, the image scale, and the positioning of object target points was that the sensitivity of the network should be such that

multi-point sub-centimetre displacements could be detected with at least a 90% confidence level.

2.2.1 Network Design

In planning a photogrammetric network for a specialized application such as deformation monitoring, due attention must be paid to the quality of the network design. Four interrelated problems need to be solved in an optimal manner at the design stage. These are the datum, configuration, weight, and densification problems. As has been shown by Fraser (1983b; paper number 4 in the external appendix), only two of these design problems typically warrant close attention in photogrammetric network optimization.

The zero-order design or weight problem involves finding an optimum form of the covariance matrix of object target point co-ordinates (C_{x_2}) for a given imaging geometry and covariance matrix of observed image co-ordinates. It should be recalled that no independently surveyed control was employed in the Turtle Mountain photogrammetric monitoring scheme, since such control needs to be established by contact measurements in order to yield sufficiently high point positioning precision. In the absence of control, the deformation monitoring network becomes one of "relative" type, where all targets are assumed liable to movement. In the zero-order design stage one seeks to define an optimum origin, orientation, and scale of the object point (X,Y,Z) co-ordinates. There are two fundamental approaches to solving the datum problem in "relative" deformation networks. The first of these employs the so-called S-transformations (see van Mierlo [1981]; paper number 6 in the appendix), whereas the second follows the more computationally straightforward approach of inner-constraint, free network adjustment. Under the latter scheme an optimum covariance matrix C_{x_2}, which is optimum in the sense that the mean variance of (X,Y,Z) co-ordinates is a minimum, is obtained directly from the least-squares adjustment process (for further details see Fraser [1983a]; paper number 2 in the appendix).

The first-order design or configuration problem is concerned with the search for an optimal network geometry, given both the precision

of the observations and criteria for the structure of $\underline{C}_{x_2}$. Questions such as the following need to be answered in the first-order design process:

1. How many photographs should image the target array?
2. What imaging geometry should be adopted?
3. How many target points are needed
4. What is the optimum photographic scale?
5. What camera (i.e., what focal length) should be used?
6. Is self-calibration warranted?

Through the process of network simulation a first-order design is carried out so as to yield a satisfactory covariance matrix $\underline{C}_{x_2}$.

A few physical contraints apply to the design of a photogrammetric monitoring network for Turtle Mountain. Low-level, slow-speed flying in the front ranges of the Rocky Mountains can be--and frequently is--a hazardous operation. This fact, coupled with the need to minimize image motion to an acceptable level, led to the selection of a minimum design flying height of 320 m above the South Peak (i.e., an altitude of about 2480 m). A standard mapping camera of 152 mm used at this height yields an image scale of about 1:2100. Initially, the planned networks were designed around this photographic scale, such that there would be a six-fold coverage of each project target point on the mountain. Accordingly, the camera stations would be situated approximately as shown in Figure 3.

Also shown in Figure 3 are the design locations of 24 object target points. As well as affording the detection of outward motions at Crack 1, in accordance with the principal geotechnical hypothesis, the object points are positioned so that relative movements between different broken rock segments of the South Peak can be detected. The actual positioning of the object target points is a fairly arbitrary procedure at the design stage, and considerable point location leeway can be tolerated before the geometric strength and sensitivity of the photogrammetric network are noticeably influenced.

With the adopted imaging configuration mentioned above, a full network simulation was conducted. From the results of this pre-analysis,

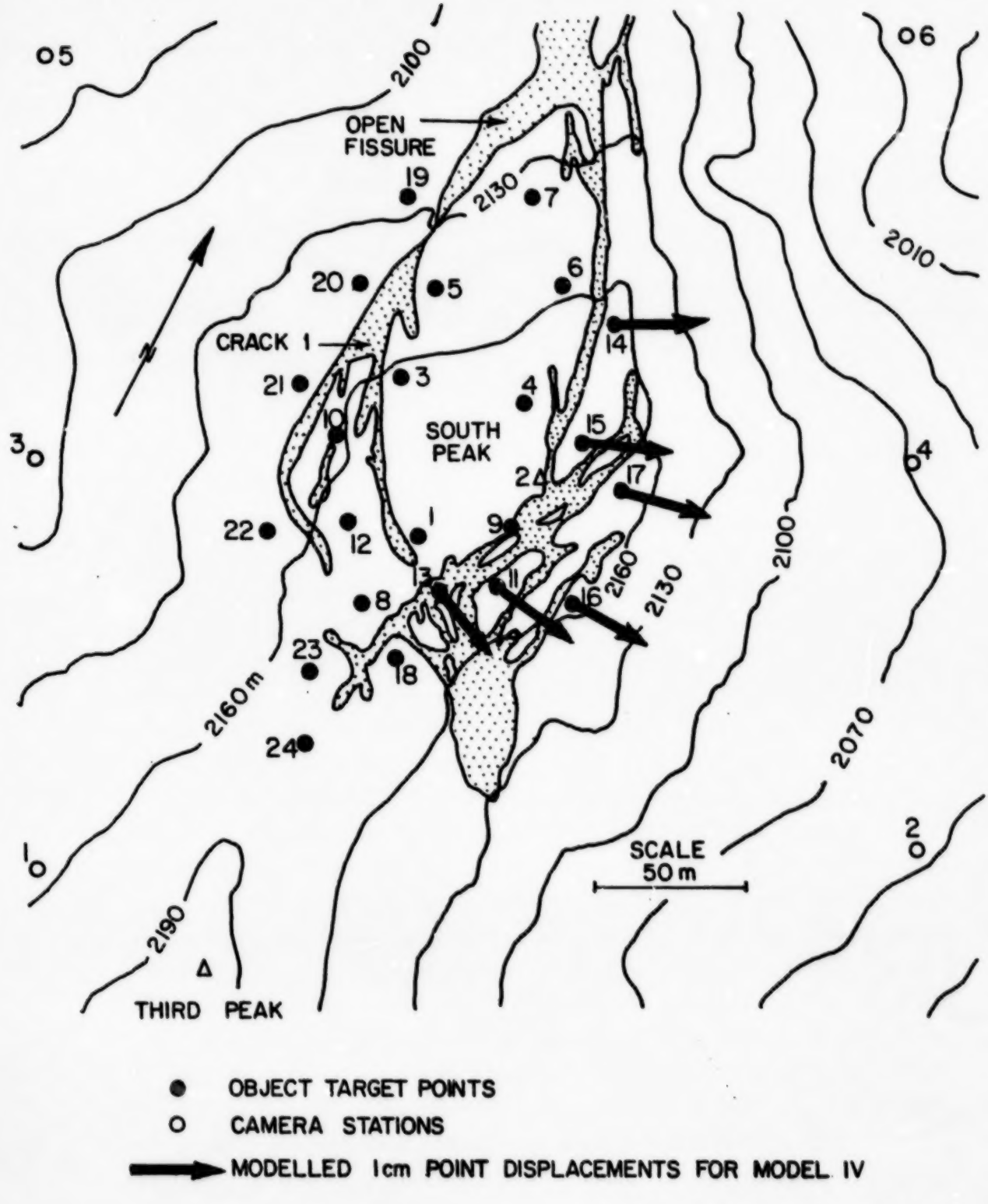

Figure 3. Simulated photogrammetric network for the monitoring of Turtle Mountain.

which are summarized in Table 1, it was apparent that a six-photo, 24-point network flown at an image scale of about 1:2000, could yield object point (X,Y,Z) co-ordinates to an accuracy of a few millimetres if the image co-ordinates could be read to a precision of 2 μm or better. Since the principal design criterion was that the network should be capable of detecting movements at the one-centimetre level, the simulated design was deemed to be satisfactory.

Implicit in the simulation conducted was the assumption that all target points would appear on each photograph. Unfortunately, the topography of the South Peak area is such that this would be unlikely to happen with only a six-photo coverage. It was principally for this reason that analysis of the data from the measuring epochs 1 and 2 used 11- and 15-photo networks, respectively. This extra coverage unquestionably enhanced both the network precision and reliability.

2.2.2 Sensitivity Analysis

Of crucial importance in deformation analysis is the sensitivity of the photogrammetric network to critical deformations. Under the assumption that there is prior information regarding the magnitude, direction, and extent of expected deformations, the network design must be such that these deformations can be detected at a certain confidence level. Measures of deformation are relative in nature (i.e., they are usually functions of positional differences which have occurred between two or more measuring epochs). It is therefore not surprising that the covariance matrix $\underset{\sim}{C}_{x_2}$ plays a key role in assessing how sensitive a network is to the detection of systematic point displacements which are likely to occur under formulated deformation models. The mathematical and statistical backgrounds of sensitivity analysis are outlined in Fraser (1983a).

For the Turtle Mountain study, the sensitivity analysis approach based on network congruency testing was adopted. At the design stage, five different deformation models were examined, these having been formulated in accordance with the geotechnical hypothesis that movements would occur either at Crack 1, or within the pyramid block. Table 2

Table 1. Bundle adjustment results for the simulated Turtle Mountain photogrammetric monitoring network.

Mean standard error $\bar{\sigma}_c$	± 0.0022 m
Square root of the ratio λ_1/λ_{65} of the largest over the smallest eigenvalue of $\underline{C}_{x_2}$	2.7
RMS value $s_{x,y}$ of image co-ordinate "measurements"	± 2.2 m

Table 2. Magnitudes of critical point movements corresponding to the five deformation models (at probability levels of $\alpha = 0.05$ and $\gamma = 0.8$).

Models	Number of Points Subjected to Movement	Magnitude of Critical Movement (mm)
I	1 (pt. 14)	17
II	1 (pt. 13)	16
III	2 (pts. 14 and 15)	13
IV	6 (pts. 11 and 13-17)	9
V	18 (pts. 1-18)	9

lists the points subjected to movement under each of these deformation models, along with the magnitudes of critical movement. Of the models, number V corresponds to the principal geotechnical hypothesis that the whole South Peak block will move outwards, thus causing a dilation at Crack 1. The remaining models serve in an examination of the sensitivity of the proposed monitoring network to single and multiple point movements. The one centimetre point displacement vectors shown in Figure 3 correspond to model IV, and also include the anticipated movements under models I, II, and III.

As anticipated, the sensitivity analysis of the simulated network indicated that single-point movements were least detectable, but the displacements of multiple points could be detected at the one centimetre level. Thus, the photogrammetric network was sensitive enough to detect deformations as small as three to four times the mean positional standard error $\bar{\sigma}_c$ of the object point co-ordinates.

As a result of the findings of the sensitivity analysis, the simulated network shown in Figure 3 was adopted as the basic design for the imaging geometry at each measuring epoch.

2.3 OBJECT POINT TARGETTING AND CONTROL SURVEY

One feature of very high precision photogrammetry is that artificial targets, as opposed to natural feature targets, are virtually always necessary. Invariably in such applications, image-pointing precision should be at the 1 to 2 μm level. Thus, topographic mapping practices of point transfer are not appropriate. For the Turtle Mountain monitoring network, 40 cm metal discs served as targets. Each disc was painted black, with a white circular central area of 12 cm in diameter. At an image scale of approximately 1:2000, the inner circle has a diameter of about 60 μm. All targets were bolted to the underlying rock to ensure long-term stability.

Although a total of 26 photogrammetric targets were positioned on the summit ridge, only 23 clearly identifiable points were imaged on the photography. Three of these were "crosses" from previous mapping projects, one near Third Peak, one on South Peak, and one in the saddle

to the north of South Peak. The locations of the 23 targets are shown on the enclosed photomap, and in Figure 4 the 20 target points used in the photogrammetric network at epoch 1 are indicated. Point number 14, which is situated near Third Peak, was eliminated from the networks because it only appeared on two photographs at epoch 1, and two further targets were not sufficiently identifiable because they were on excessively steep sloping rock. Because the optical centre of the mapping target, point 101, was not definable, this point was not included in the photogrammetric network at epoch 2.

The use of survey control can enhance the overall positional accuracy of a photogrammetric network. However, if such additional control is to be imposed, it is crucial that the accuracy of the "fixed" parameters be measurably higher than the photogrammetric-positioning precision.

Some levelling data were provided by Alberta Environment following the summer field measurements in 1982, but when these data were adjusted simultaneously with the photogrammetric network a serious distortion of shape occurred. At first it was thought that the introduced errors were due to uncertainty about which photo targets corresponded to which levelling points. However, it was later discovered that a significant error had gone undetected in the level traverse. Following this, no additional survey control or field measurements were introduced into the photogrammetric networks at epochs 1 and 2. Initially, the network at epoch 1 was adjusted with a datum defined by the (X,Y,Z) co-ordinates for the panelled crosses on South and Third peaks, and a height for point number 10. The adoption of this arbitrary control may mean that there is a slight difference in scale, orientation, and origin with respect to the geodetic datum, but this is of no concern for the deformation monitoring.

A further reason for not employing any additional surveying measurements was the fact that what was sought was a remote, non-contact monitoring scheme. Yet to establish a surveying network to sufficient accuracy on the summit ridge, contact measurement would be required.

2.4 PHOTOGRAPHY

Specifications for the photographic coverage of an object target array are established at the network design stage. As is discussed in Section 2.2, two parameters are of central importance for low-level aerial photography. The first is imaging scale since this directly influences network positioning accuracy, the second is the tolerance level set for image motion. One usually seeks a balance between the design demands of these two parameters. If an aeroplane is at its slowest working airspeed, the degradation of image quality caused by image motion is directly proportional to the photographic scale. Lowering the flying height to achieve enhanced accuracy through larger scale photo coverage can increase image motion to an unacceptable level.

In the context of deformation monitoring it is also desirable to use, as far as possible, the same imaging geometry and the same camera at each measuring epoch. This enhances the chances of eliminating those components of systematic error which are common to the camera system. Both aerial photographic missions carried out for the Turtle Mountain monitoring employed the same camera, a Wild RC8 mapping camera of 152 mm focal length. The design specifications called for an average image scale of about 1:2000 (i.e., a flying height above ground of approximately 310 m), and also a maximum airspeed of around 80 knots to keep image motion down to an acceptable level. Because of extremely difficult flying conditions, these specifications were not entirely met, but reasonable photography was obtained. Brief details of the photographic coverage at each of the two epochs are given in the following two sections.

2.4.1 Epoch 1 (1982)

At the time the photography was flown it was not possible, because of excessive turbulence, to fly at lower than about 2500 m (300 m above the South Peak). Thus, the planned coverage of 1:2000 photography was not obtained. From the strips of photography, eleven images were useful for the photogrammetric point determination: seven photos from the two strips flown at an elevation of about 2520 m (a scale of approximately 1:2240 at the mean target elevation) and four photos from

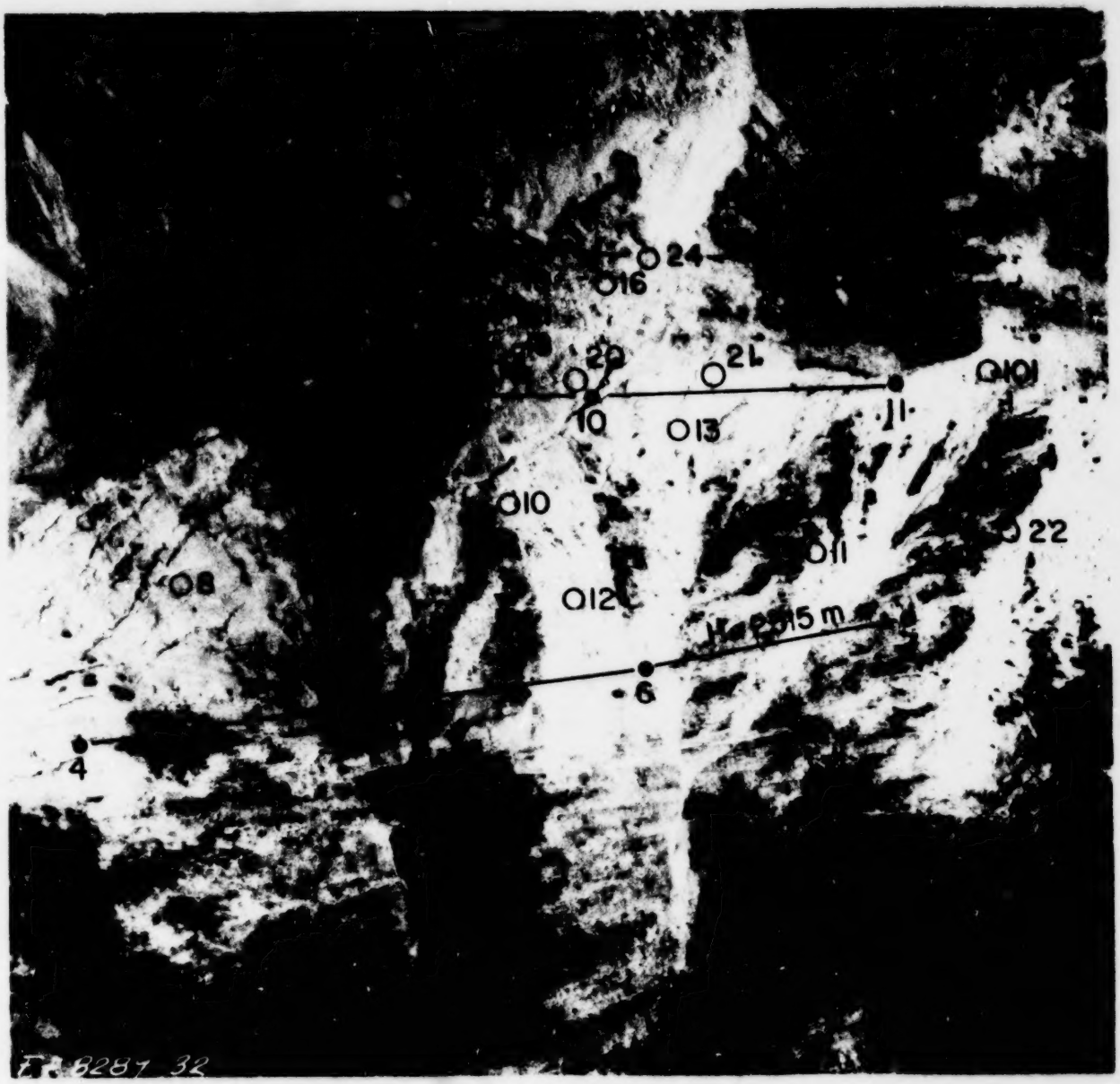

Figure 4. Photogrammetric target array and camera station locations at Epoch 1.

a strip flown at 2580 m (≈ 1:2630), as shown in Figure 4. Not all targets were imaged on all photographs, but at least six imaging rays were available for space intersection at each object point.

2.4.2 Epoch 2 (1983)

As had occurred with the photography at epoch 1, it was once again not possible to fly as low as the design specification called for. Eleven camera stations from three strips of photography at epoch 2 were sufficiently coincident with corresponding exposure positions at epoch 1. In addition, to overcome the weaker than desirable imaging geometry encountered at epoch 1 in the area from point 24 to 25, four additional exposures were utilized in the epoch 2 network. These camera stations, numbered 12 through 15, are shown in Figure 5. Also shown in the figure are the average flightline elevations. Note that the mean photographic scale is somewhat less for the 1983 photography when compared to that obtained in 1982. Three strips were flown at about 2580 m (≈ 1:2630), one at 2590 m (≈1:2700), and one at 2610 m (≈1:2830).

2.5 PHOTOGRAMMETRIC POINT MENSURATION

It is imperative for high-precision photogrammetry that image point measurements be carried out to the highest practicable accuracy. As is shown in Fraser (1983b), the final precision $\bar{\sigma}_c$ of the object point (X,Y,Z) co-ordinates is directly and linearly related to the mean standard error σ of image co-ordinates (i.e., $\bar{\sigma}_c = k_\delta$ where k is a constant for any network). Most commonly, a σ-value of 1 to 2 μm is sought, and this implies that a first-order analytical plotter or comparator needs to be used. Multiple co-ordinate readings, say 2 to 4 times, are also highly desirable, and measurements should be made on the original film negatives.

All the Turtle Mountain photography was measured monoscopically in a Wild AC/1 analytical plotter at The Orthoshop in Calgary (stereoscopic measurement proved to be too slow due to the large height variations between object points). Multiple image (x,y) co-ordinate

measurements were made at each target point, with the estimated standard error being $\sigma \simeq 2$ μm.

2.6 ADJUSTMENT OF PHOTOGRAMMETRIC NETWORKS

The photogrammetric data from each measuring epoch were restituted by a free-network bundle adjustment technique in which the method of inner constraints was applied (see Fraser 1983a,b). For high-precision photogrammetric networks, use of the bundle method--sometimes with self-calibration--is mandatory. Unless S-transformations are to be employed in the deformation analysis, it is also essential to use a free-network adjustment when the monitoring network is of "relative" type. From the adjustment process, two quantities are required for later analysis: the vector $\underline{x}_2$ of estimated object point (X,Y,Z) co-ordinates and the corresponding covariance matrix $\underline{C}_{x_2}$. Since the majority of commercially available bundle adjustment software packages for aerial trianguiation do not compute $\underline{C}_{x_2}$, and to the author's knowledge none permit free-network adjustment, such programs are not appropriate for use in a monitoring system such as the one developed for Turtle Mountain.

The results obtained for the two network adjustments are summarized in Table 3. Both networks exhibit approximately the same level of precision, $\bar{\sigma}_c \simeq \pm 4$ mm. Also, the homogeneity of precision, as expressed by the eigenvalue ratio, is roughly the same at each epoch. The falloff in precision which accompanies the smaller image scale at epoch 2 is counterbalanced by both the influence of the additional photographic data and the smaller RMS value of image co-ordinate residuals.

Both the photogrammetric networks display somewhat poorer precision than did the intitial simulated configuration. Two principal factors contribute to this. The first is that the design imaging scale could not be achieved at the times of photography, and the second is the larger maximum height variation between target points in the object point array established. The height variation between points 18 and 8 is about 100 m, which is in excess of 25% of the average flying height above

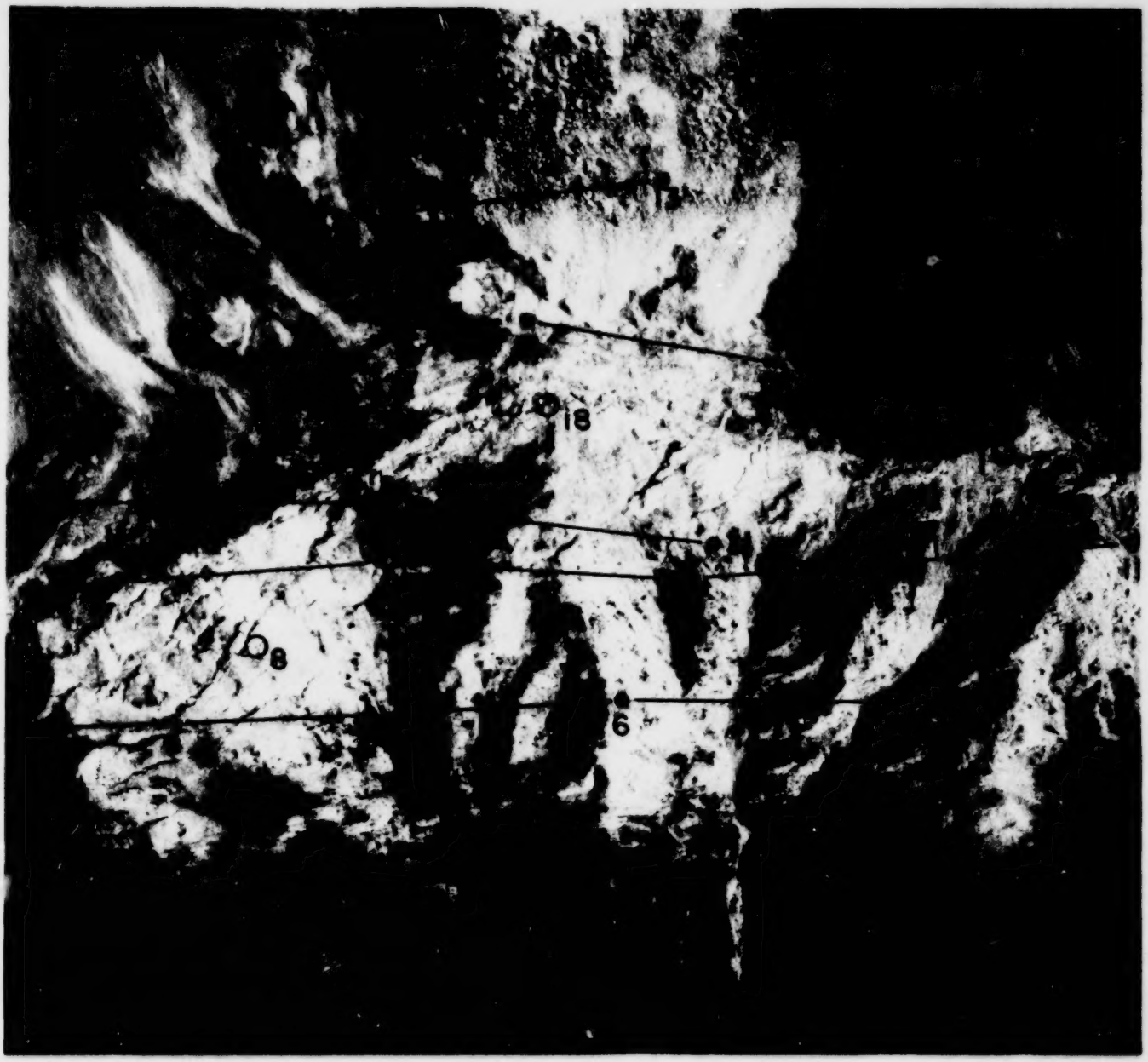

Figure 5. Photogrammetric imaging geometry for Epoch 2.

Table 3. Summary of photogrammetric free-network adjustment results for epochs 1 and 2. Inner constraints relate to the same 11 points in each network (i.e., they have the same datum).

	Epoch 1	Epoch 2
Average image scale	1:2 300	1:2 680
Number of photographs	11	15
Number of target points	20	19
RMS value $s_{x,y}$ of image co-ordinate residuals	± 2.2 µm	± 2.1 µm
Mean standard errors: $\bar{\sigma}_c$	± 4.1 mm	± 3.9 mm
$\bar{\sigma}_{X,Y}$	± 2.9 mm	± 2.7 mm
$\bar{\sigma}_Z$	± 5.8 mm	± 5.6 mm
Square root of the ratio of the largest over the smallest eigenvalue of $\underline{C}_{x_2}$	8.7	9.1
Degrees of freedom	223	312

ground at each epoch. This variation in the "depth" of the target array accounts for the magnitude of the eigenvalue ratios listed in Table 3. Notwithstanding the less than optimum results attained, both networks still displayed sufficient sensitivity to detect multiple point movements at the centimetre level (see Fraser and Stoliker 1983; paper number 3 in the external appendix).

Table 4 lists the adjusted X, Y, and Z co-ordinates of the 20 deformation monitoring points at epoch 1, along with their respective standard errors. It must be recalled that the (X,Y,Z) Cartesian system selected as the reference co-ordinate frame is only in approximate coincidence with the (E,N,h) projection co-ordinate system which has been used to co-ordinate a number of survey marks on the summit ridge of Turtle Mountain.

2.7 DEFORMATION ANALYSIS

Central to any deformation analysis is the proof of the existence or non-existence of point movements. Since neither "true" co-ordinates nor "true" deformations can be obtained through a physical measuring process it is necessary to turn to statistical testing of "estimated" deformations in order to prove whether significant movements have occurred between two measuring epochs. Generally, the formulated null hypothesis which is tested is that network points have not moved. If this hypothesis passes the linear hypothesis test at the chosen confidence level (usually 90% or 95%), the assumption that no significant deformation in either the network shape or size has occurred is accepted. Essentially, the congruency of the two networks is examined within the tolerance implied by their respective covariance matrices.

Rejection of the null hypothesis implies that significant deformations have occurred, and it is then necessary to examine both the localized nature of the point movements and the trends in the resulting strain field.

Table 4. Adjusted X, Y, and Z co-ordinates of the 20 photogrammetric target points at epoch 1, with their standard errors.

Point Number	X (m)	Y (m)	Z (m)	σ_x (mm)	σ_y (mm)	σ_z (mm)
8	10162.152	10370.383	2104.589	2	4	5
9	10148.800	10268.684	2132.489	2	2	4
6	10201.773	10286.164	2129.265	2	2	5
4	10195.978	10243.798	2153.191	2	2	4
10	10097.946	10209.111	2163.681	2	2	4
12	10040.578	10210.573	2125.842	2	2	5
13	10079.280	10138.006	2167.485	2	2	5
21	10088.142	10102.707	2190.093	2	2	5
20	10126.477	10154.491	2186.368	2	2	4
18	10166.891	10161.266	2198.923	2	3	3
181	10169.189	10157.598	2199.370	2	3	4
19	10174.923	10141.120	2195.725	2	2	4
17	10178.166	10128.012	2185.017	2	2	4
16	10147.228	10111.499	2179.751	2	2	4
24	10145.691	10093.396	2158.053	3	2	6
11	9984.492	10112.868	2143.837	3	3	7
25	10048.690	9989.617	2182.681	2	3	6
1	10016.674	10006.200	2204.127	2	3	5
101	10016.898	10006.916	2203.758	3	4	8
22	9945.846	10037.151	2171.486	4	2	6

The approach to deformation analysis adopted in the Turtle Mountain monitoring project is comprised of three interrelated phases:

1. global congruency testing of the network;
2. localization of deformations in space and time; and
3. testing the network, if it has been deformed, for significant components of homogeneous strain.

2.7.1 The Global Congruency Test

Fundamentally, this test examines the null hypothesis that the object target point array is stable over all measuring epochs. For the two-epoch analysis of the Turtle Mountain photogrammetric measurements, the null hypothesis H_o can be written

$$H_o : E\{\hat{\underline{x}}_2\} - E\{\hat{\underline{x}}_1\} = E\{\hat{\underline{d}}\} = 0 \qquad (3)$$

where $\hat{\underline{x}}_2$ is the vector of three-dimensional object point co-ordinates at epoch i, and $\hat{\underline{d}}$ is the vector of co-ordinate differences. A standard F-test, in which the quadratic form of the deformations is compared to the a posteriori variance factor, determines whether H_o will be rejected. Due to the fact that the covariance matrix of $\underline{d}$ has a rank defect of seven, a pseudo-inverse of this matrix is employed in the computation of the quadratic form of the deformations. For complete details of this test the reader is referred to the reports by Niemeier (1981), van Mierlo (1981), and Stolliker (1982) in the appendix.

Figures 6 and 7 show the target point co-ordinate differences which occurred in the horizontal and vertical directions between epochs 1 and 2. The magnitudes and directions of these "point movements" are datum-dependent quantities and thus they cannot be interpreted initially as actual deformations. The determination of point displacements occurs in the localization phase. The individual co-ordinate differences shown in the figures form the $\underline{d}$ vector and although they do not necessarily reflect true movements, one can infer from their magnitudes something about those points which likely did move.

On applying the global congruency test to the vector $\underline{d}$ obtained, it was found that the test failed at the 95% confidence level.

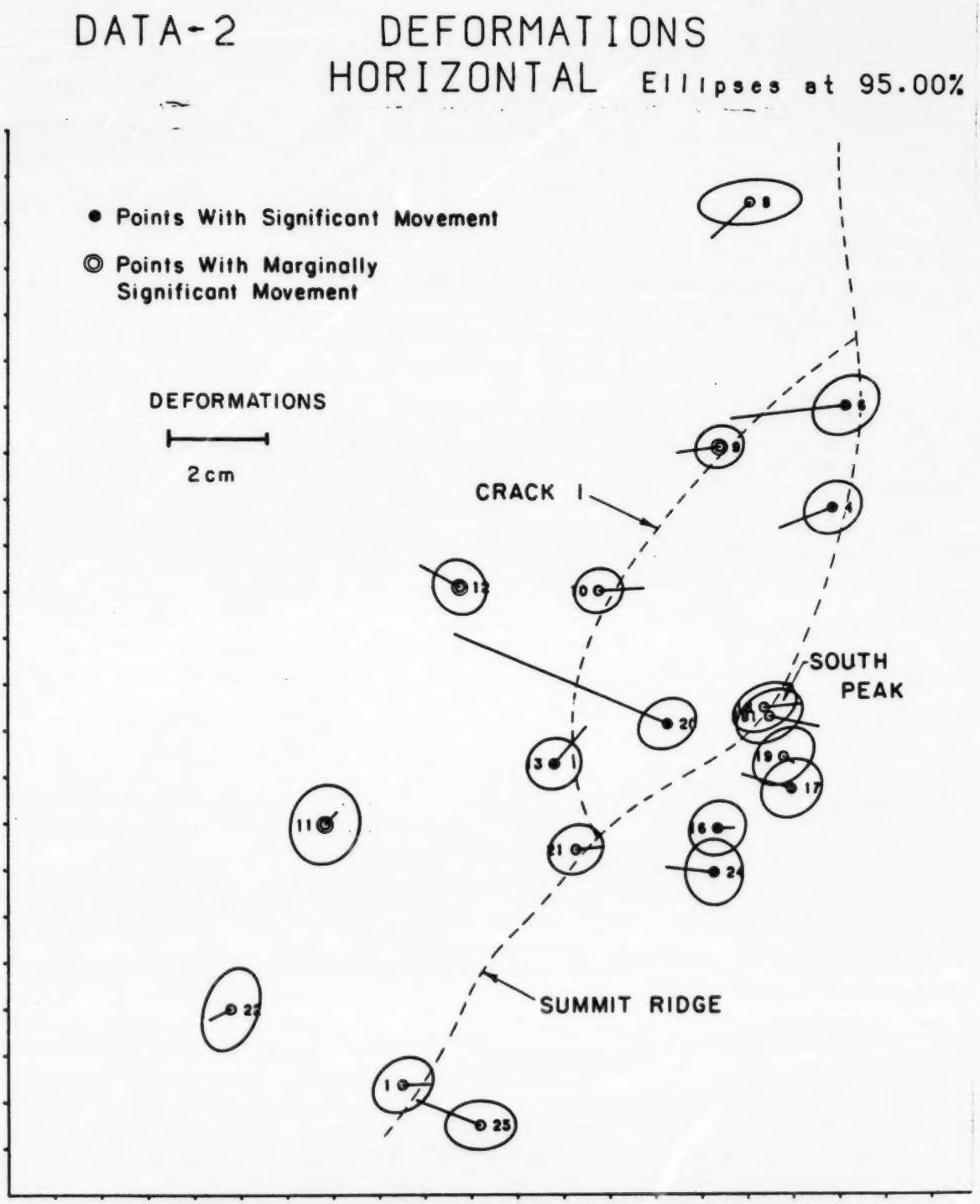

Figure 6. "Deformations" in the horizontal plane, as determined by the localization procedure. The inner constraint datum comprises 11 points, none of which are located on the South Peak side of Crack 1.

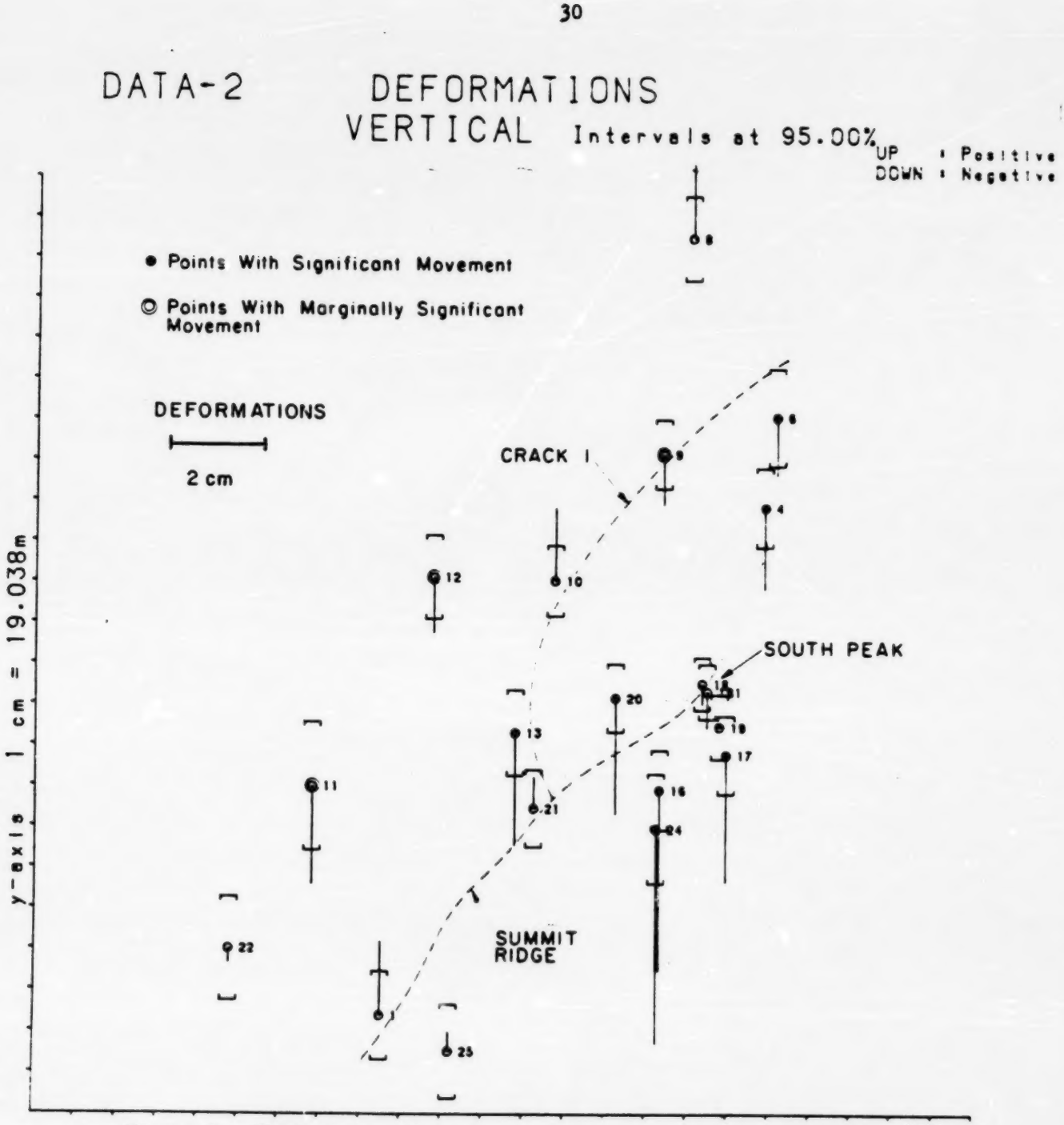

Figure 7. "Deformations" in the vertical direction, as determined by the localization procedure. The inner constraint datum comprises 11 points, none of which are located on the South Peak side of Crack 1.

Rejection of the null hypothesis is then accompanied by the conclusion that between epochs 1 and 2 a significant change in shape occurred in the object target point array on Turtle Mountain.

2.7.2 Localization of Deformations in Space and Time

Having determined that significant deformations occurred (i.e., the global congruency test failed) it is necessary to isolate the point movements in both the time and geometry domains. In the case of Turtle Mountain only two epochs of measurement have thus far been carried out, and so a localization in time is not required. However, the question of which movements caused the target point network to significantly change shape must be addressed.

Point displacement localization in a "relative" deformation situation is a reasonably complex procedure. A comprehensive treatment of the problem is given in van Mierlo (1981), and for the Turtle Mountain investigation a software package compiled by Gruendig et al. (1982) has been employed. The procedure is as follows:

Step 1. An S-transformation is carried out on both $\underline{x}_{2_i}$ and $C_{\underline{x}_{2_i}}$ for the networks of each of the two epochs being compared. This transformation yields a computational base (datum) which includes only "stable," common points. Of course, since on the first pass through step 1 no point movements have been isolated, the datum includes all the points common to each epoch.

Step 2. After the S-transformation, a congruency test is performed to test the stability of the sub-section of the target array that does not include points with significant movement. On the first pass through step 2, the test performed is the global congruency test. But for subsequent passes, moved points are "eliminated." If the test fails, further significant point (or block) movements are still to be identified. If it passes, the points remaining in the computational base are deemed to be stable. "Eliminated"

points are those at which significant deformation occurred. The localization process is then complete.

Step 3. On the failure of the test in step 2 to pass, that sub-vector of $\underline{d}$ (for a point or block of points) which has the largest contribution to the quadratic form $\underline{d}^T \underline{C}_d \underline{d}$, where $\underline{C}_d$ is the current covariance matrix of $\underline{d}$, is deemed to represent a significant deformation. The point (or block) is then flagged for "elimination" and removed from the current subset of "stable" points. Following this, step 1 is again repeated.

For the localization of single-point movements, steps 1, 2, and 3 are progressively repeated until such time that the datum contains only stable points. The point movements detected then have exactly the same magnitudes as those which would be determined if the two network adjustments were repeated using a partial inner constraint (datum) that included only the "non-eliminated" points.

Table 5 summarizes the results of the deformation localization computations carried out for epochs 1 and 2. The first eight points listed (above the solid line) were found to be stable. The last eight points (below the dashed line), on the other hand, were those at which significant movements had taken place. The sequence of point location is from the bottom up (i.e., point 20 was "eliminated" first, then point 24, and so on up to point 9). Although points 9, 11, and 12 were found to have significantly moved, the test results were very marginal. Thus there is some question as to whether the point displacements represent an actual movement or the effects of random error propagation.

Through a further statistical test it is possible to verify the individual deformations which result from the localization procedure. Under the assumption that estimated object point positions are not highly correlated, a three-dimensional test can be carried out to examine the hypothesis that the individual co-ordinate differences ΔX_i, ΔY_i, and ΔZ_i of point i are zero. This test was conducted for the estimated point displacements which resulted from the two separate network adjustments. At a significance level of 0.05, two of the three marginal deformations passed the test, but point number 9 did not. As a result of this confirmation of the localization results, the points 11 and 12 were

Table 5. Summary of deformation analysis results for epoch 2 versus epoch 1. Point movement magnitudes are indicated by d.

Point Number	ΔX (cm)	ΔY (cm)	ΔZ (cm)	d (cm)	Significant deformation? localization	t-test
8	- .6	- .8	.4	1.1	no	no
181	.6	.1	- .9	1.1	no	no
19	- .2	.1	.2	.3	no	no
10	.7	.2	.8	1.1	no	no
1	- .1	.1	1.4	1.4	no	no
18	.3	.4	- .6	.8	no	no
21	.1	.2	.4	.4	no	no
22	- .9	- .3	-1.6	1.8	no	no
9	- .9	- .1	-2.2	2.4	yes	yes
12	- .9	.4	-2.9	3.0	yes	no
11	0	.1	-3.8	3.8	yes	no
4	-1.2	- .3	-2.4	2.7	yes	yes
13	.4	.9	-3.5	3.6	yes	yes
16	.1	.1	-4.4	4.4	yes	yes
25	-1.8	.5	.4	1.9	yes	yes
17	-1.4	.5	-2.9	3.3	yes	yes
6	-2.4	- .2	-2.0	3.2	yes	yes
24	-1.3	.1	-5.2	5.3	yes	yes
20	-5.0	2.1	-3.2	6.3	yes	yes

deemed to be stable, whereas point 9 was assigned to the group which exhibited significant point displacements.

Having determined the significant single point displacements, it is useful to examine whether any group (i.e., block) movements occurred. By referring to Figures 6 and 7, it can be seen that two three-point groupings could have undergone a block translation, with the principal movement being a settlement of 3 to 5 cm in one case and 2 cm in the other. Both the group movements of points 4, 6, and 9, and 16, 17, and 24 were found to be statistically significant.

The most significant single-point movement located was point 20 which was estimated to have been displaced by 6.3 cm in an approximate azimuth of 246°. As it turned out, this target was physically relocated by Alberta Environment personnel, and the extent of movement was not made available to the author--nor indeed was the point number of the relocated point--until after the localization procedure was completed. From surface distance measurements and a compass reading, it was determined that the target was shifted 6.2 cm in an azimuth of around 250°. Thus, the independent check on the photogrammetric measurement revealed a discrepancy of 1 mm, which is a surprisingly accurate result. The 95% confidence region associated with point 20 is approximately a circle of 5 mm radius in the horizontal plane, and in the vertical the 95% region extends to about ±10 mm.

2.7.3 Combined Adjustment of Both Photogrammetric Networks

The findings of the localization process were that, while 10 targets remained stable, 9 points underwent significant movement. As a final check on the results it is possible to combine all the photogrammetric data into a single network, and then adjust this combined network. Points in epoch 2 at which deformation took place are assigned new numbers and the resulting adjusted distance between each of the newly numbered points and its corresponding position in epoch 1 (effectively a separate point) indicates the target point's movement.

A total of 26 photographs and 29 points (20 original and 9 renumbered in epoch 2 data) formed the combined Turtle Mountain network.

Figures 8 and 9 illustrate the point displacements determined by the combined adjustment, as well as the overall precision obtained (error ellipses in the horizontal and a confidence region bound in the vertical). Although minor discrepancies exist between the deformation pattern obtained in the localization process and the displacements shown in Figures 8 and 9, the point movements are in close overall agreement. A component of the difference in estimated deformations comes from the inclusion of points 11 and 12 as stable points. Thus the movement at these targets is constrained to zero in the combined network.

2.7.4. Strain Analysis

In the case of Turtle Mountain it was thought that the determination of strain components may contribute to a better understanding of the mechanisms of any deformation that is occurring (e.g., strain due to water pressure and flow). For the determination of the rates of homogeneous infinitesimal strain the method proposed by Brunner (1979) (paper number 1 in the appendix) has been adopted. Under this approach deformations are assumed to result from an affine transformation in a homogeneous strain field which covers either all or part of the object point network. The strain components of extensions along each co-ordinate axis and shear in each plane, and the components of rigid body rotation about each orthogonal axis are then related to the estimated deformations (co-ordinate differences) by

$$\hat{\underline{d}} = \underline{B}\,\underline{u} \qquad (4)$$

where $\underline{B}$ is the coefficient matrix of the incremental three-dimensional affine transformation (see Brunner 1979) and $\underline{u}$ is the vector of strain parameters, given as:

$$\underline{u}^T = (\varepsilon_{XX}, \varepsilon_{YY}, \varepsilon_{ZZ}, \varepsilon_{XY}, \varepsilon_{XZ}, \varepsilon_{YZ}, \omega_{XX}, \omega_{YY}, \omega_{ZZ}) \qquad (5)$$

Extension along the k-axis is indicated by ε_{kk}, shear in the jk-plane by ε_{jk} and rotation about the k axis by ω_{kk}. In the typical case where

DATA-1+2 DEFORMATIONS
HORIZONTAL Ellipses at 95.00%

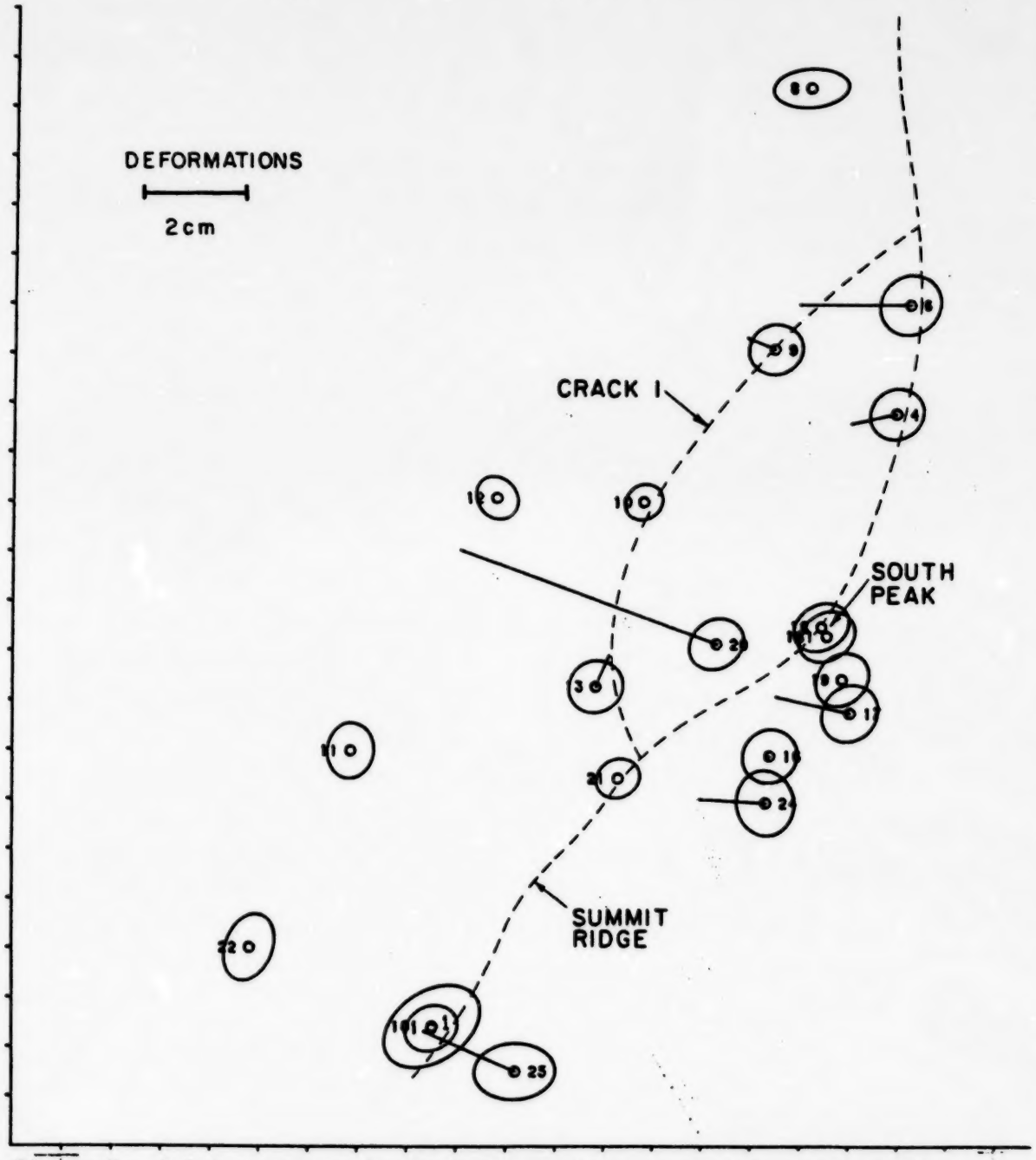

Figure 8. Point movements in the horizontal plane, as determined in the combined network adjustment.

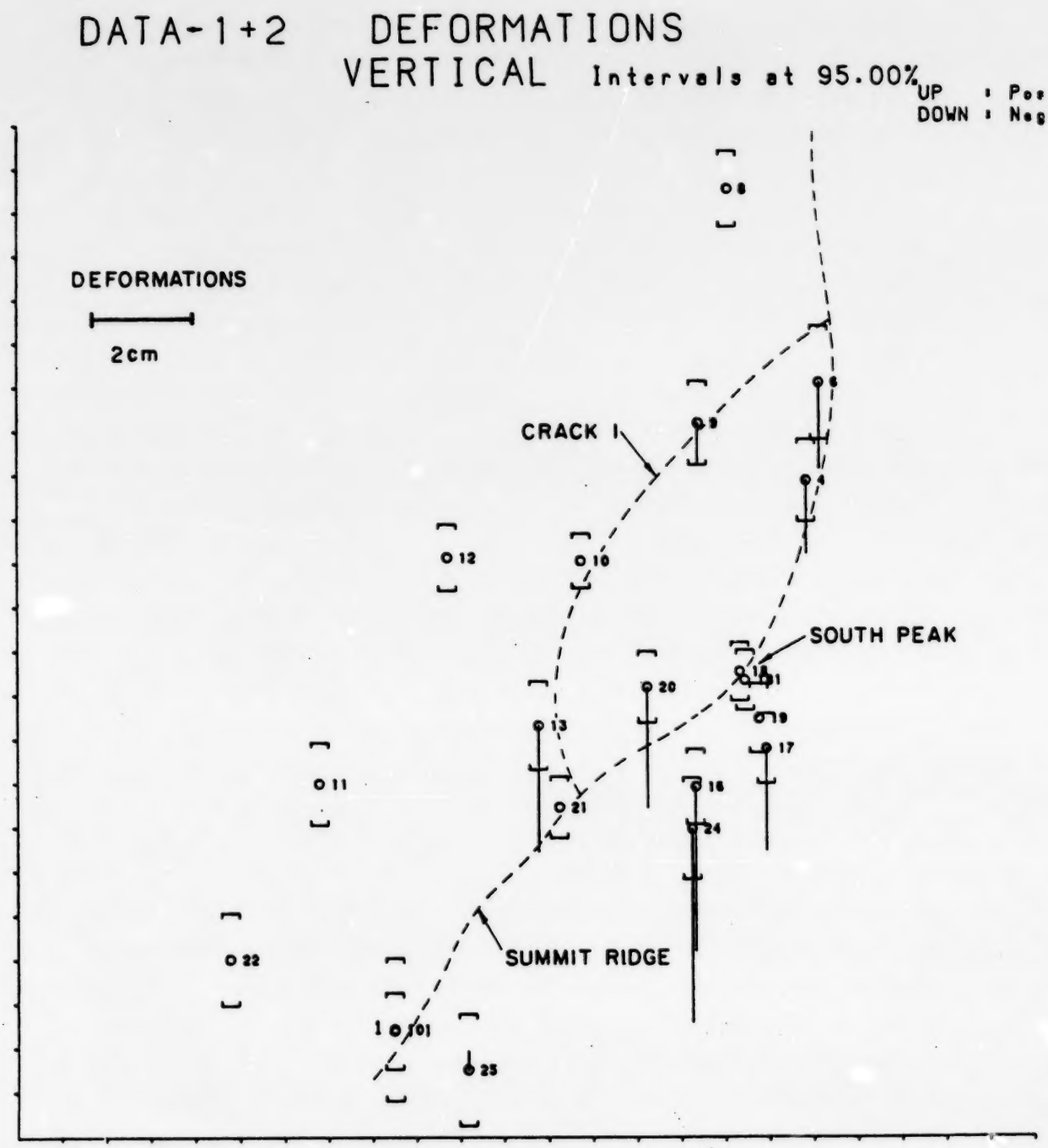

Figure 9. Point movements in the vertical direction, as determined in the combined network adjustment.

there are in excess of three object points, the method of least squares is adopted for the solution of $\underline{u}$. Again, because of the defect of rank of the covariance matrix of $\underline{d}$, a pseudo-inverse is used in the solution of the resulting normal equations. From $\underline{u}$, both principal strains and the volumetric strain can be computed.

Following the computation of $\underline{u}$, the null hypothesis of strain field homogeneity can be tested with an F-test analogous to the congruency test for significant deformation. Further, it is also possible to ascertain whether the strain components are statistically significant at a chosen confidence level. Because of the high correlation which can be encountered between the nine parameters forming $\underline{u}$, it is often necessary to adopt multi-dimensional rather than one-dimensional tests to ascertain whether the estimated values of selected strain components are significantly different from zero.

Not surprisingly, the strain analysis of the deformation pattern indicated in Figures 8 and 9 did not reveal the presence of statistically significant homogeneous strain. This was principally due to the isolated nature of some of the point displacements. At the time of writing, no analysis had been conducted using subgroups of the object target array, but work on this aspect continues.

2.8 INTERPRETATION OF RESULTS

Based on the results obtained in this investigation it can be concluded that portions of the South Peak area of Turtle Mountain are subject to deformation. In the one-year period between the summers of 1982 and 1983, target point movements of a few centimetres and greater occurred at eight locations on the summit ridge (point 20 is not included since it was physically relocated). Although there is a marked horizontal displacement of the two groups of points formed by targets 4, 6, and 9, and 16, 17, and 27, the main component of movement appears to be vertical settling.

In this the measuring phase of the overall Turtle Mountain monitoring program, no attempt has been made to interpret the geotechnical significance of the estimated deformations. However, the

point movements obtained do not tend to support the hypothesis that the six million cubic metre rock wedge bordered by Crack 1 is moving as a block, if it is indeed moving at all.

3. CONCLUSIONS

The basic criterion governing the design of the photogrammetric monitoring system for Turtle Mountain was that the deformation analysis procedure should be able to monitor multiple target point movements to an accuracy of one centimetre. From the results obtained for measuring epochs 1 and 2, it can be concluded that the photogrammetric networks established were of sufficient sensitivity to meet the required accuracy criteria, even though their precision was slightly below the optimum design level. Nine statistically significant point movements were located in the target array of 20 points.

Through the successful carrying out of this investigation, further weight is added to the contention that high-precision analytical photogrammetry provides an accurate non-contact, three-dimensional measuring tool which is ideally suited both to tasks such as the monitoring of deformations on Turtle Mountain, and to general structural monitoring and measurement in numerous areas of engineering.

4. RECOMMENDATIONS

With the completion of this research project a practical methodology has been established for the photogrammetric monitoring of the South Peak area of Turtle Mountain. Should this work continue, the procedures adopted should follow closely those which have been outlined in this report. In a sense, this report has aimed at providing a design memorandum in that each stage of the monitoring project is separately treated.

Although a working system has been developed and implemented, further research on the photogrammetric monitoring scheme is warranted. This additional work would embrace, initially, an extension of the deformation analysis to multiple epochs, as well as a refinement of some of the statistical models employed and a further study of the applicability of strain analysis techniques.

5. REFERENCES CITED[1]

Brunner, F.K. 1979. On the analysis of geodetic networks for the determination of the incremental strain tensor. Survey Review 25:56-67.*

Cruden, D.M. and J. Krahn. 1978. Frank rockslide, Alberta Canada. IN Rockslides and avalanches, ed. B. Voight. Vol. 1. Amsterdam: Elsevier. pp. 97-112.

Fraser, C.S. 1983a. Photogrammetric monitoring of Turtle Mountain: a feasibility study. Photogrammetric Engineering and Remote Sensing 49(11).*

Fraser, C.S. 1983b. Network design considerations for non-topographic photogrammetry. Photogrammetric Engineering and Remote Sensing. (In press.)*

Fraser C.S. and P.C. Stoliker. 1983. Deformation monitoring of a landslide area by high-precision photogrammetry. Presented to FIG XVII International Congress. June 19 to 28, 1983; Sofia, Bulgaria.*

Gruendig, L., J. Bahndorf, and M. Neureither. 1982. Zur Auswirkung von Beobachtungsfehlern auf Deformationen oder Deformationen als Beobachtungsfehler Gedeutet. Presented to FIG Comm. 6 Meeting, Munich, W. Germany.*

van Mierlo, J. 1981. A testing procedure for analysing geodetic measurements. IN: Proceedings II International Symposium on Deformation Measurements by Geodetic Methods. Editor L. Hallermann. 1978; Bonn, W. Germany. Stuttgart: Konrad Wittner.*

Niemeier, W. 1981. Statistical tests for detecting movements in repeatedly measured geodetic networks. Tectonophysics 71:335-351.*

Stoliker, P.C. 1983. CONGRU & GRAPHS: An explanation of software being developed for photogrammetric network congruency analysis. University of Calgary, Division of Surveying Engineering. (Unpublished manuscript.)*

[1] Copies of references marked with an asterisk are located in an external appendix to this report, published as RMD Report OF-62.